Autothermal reforming of simulated and commercial diesel: The performance of zirconia-supported RhPt catalyst in the presence of sulfur

Reetta K. Kaila *, Andrea Gutiérrez, A. Outi I. Krause

Helsinki University of Technology (TKK), Department of Biotechnology and Chemical Technology, P.O. Box 6100, FI-02015 TKK, Finland

ABSTRACT

Simulated and commercial low-sulfur diesel fuels ($S < 10$ ppm) were studied in autothermal reforming (ATR) on Rh and Pt and bimetallic RhPt catalysts supported on ZrO_2 with the aim of obtaining fuel gas suitable for solid oxide fuel cell applications.

In ATR of the simulated fuels, the catalysts deactivated markedly in the presence of H_2S, whereas in ATR of simulated fuels in the presence of 4,6-dimethyldibenzothiophene (4,6-DMDBT) and in ATR of commercial diesel the catalyst deactivated only slightly over several hours. In view of its different effect, H_2S cannot be considered a suitable model compound for heterocyclic sulfur compounds present in commercial low-sulfur fuels.

In ATR of commercial low-sulfur diesel, carbon formation increased with the Pt loading, whereas sulfur deposition on the catalyst was strongest on the monometallic Rh/ZrO_2. Furthermore, less carbon was deposited on the RhPt catalyst in the presence than absence of H_2S, as sulfur blocked the catalyst active sites. The catalyst could be reactivated by stopping the H_2S flow.

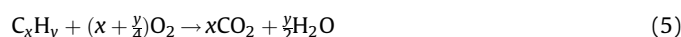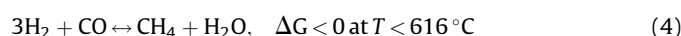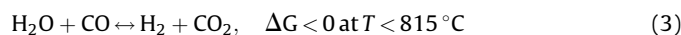© 2008 Elsevier B.V. All rights reserved.

1. Introduction

During combustion, the sulfur present in fossil fuels generates sulfur oxides, which cause air pollution and acid rain. Although most of the sulfur compounds can be removed by the present catalytic hydrodesulfurization (HDS) technology, certain hetero-cyclic sulfur compounds are difficult and expensive to remove [1,2]. Thus, "sulfur-free" fuels in fact still contain sulfur (<10 ppm) compounds after HDS treatment, in particular the dialkyl dibenzothiophenes, of which 4,6-dimethyldibenzothiophene (4,6-DMDBT) is the most stable [1,3]. The high resistance of 4,6-DMDBT to HDS processes is proposed to be due to the steric hindrance of the methyl groups, which prevent contact between the thiophenic sulfur atom and the active site of the catalyst [1,4]. The use of these commercial fuels as energy source for fuel cell systems is attractive although its sulfur content acts as a poison for the fuel cell system. The advantage of diesel fuel is its high volumetric hydrogen density [5] and the existing infrastructure [6].

The production of hydrogen-rich fuel gas from liquid hydro-carbons by autothermal reforming (ATR) is of great interest for high temperature fuel cell applications [7–11]. ATR combines endothermic steam reforming reactions (SR, Eq. (1)) with exothermic partial oxidation (POX, Eq. (2)) yielding, according to thermodynamic calculations [12], a thermoneutral total reaction that determines the final product distribution

$$C_xH_y + xH_2O \leftrightarrow xCO + \tfrac{y+2x}{2}H_2 \tag{1}$$

$$C_xH_y + \tfrac{1}{2}O_2 \leftrightarrow xCO + \tfrac{y}{2}H_2 \tag{2}$$

Water gas shift (WGS, Eq. (3)) and methanation (Eq. (4)) equilibrium reactions are possible reactions for the ATR products. In addition, unwanted side reactions may take place, such as complete oxidation (OX, Eq. (5)) and thermal cracking of the fuel. The presence of side reactions can be controlled through choice of the catalyst and optimization of the reaction conditions

$$H_2O + CO \leftrightarrow H_2 + CO_2, \quad \Delta G < 0 \text{ at } T < 815\,°C \tag{3}$$

$$3H_2 + CO \leftrightarrow CH_4 + H_2O, \quad \Delta G < 0 \text{ at } T < 616\,°C \tag{4}$$

$$C_xH_y + (x + \tfrac{y}{4})O_2 \rightarrow xCO_2 + \tfrac{y}{2}H_2O \tag{5}$$

Our previous studies have shown ZrO_2-supported bimetallic RhPt catalysts to be active and selective for H_2 formation by ATR of sulfur-free hydrocarbon mixtures in the temperature range of

400–900 °C [13,14]. Complete conversion of hydrocarbons is achieved at temperatures higher than 700 °C. Beyond 700 °C, moreover, the H_2 production predicted by the thermodynamics is reached [14].

The effect of sulfur in the reforming of liquid hydrocarbons has received considerable attention, but relatively little information is available in the literature, as noted in the recent review by Shekhawat et al. [8]. Although the sulfur tolerance of noble metal catalysts has been studied with various sulfur compounds (H_2S [2,15,16], SO_2 [17], CH_3SH [18], and thiophenes [15,19,20]) and various sulfur-containing commercial fuels (e.g. HD-kerosene [2], diesel [11], gasoline [19], and jet fuel [21]) published information on the catalysts and the sulfurous compounds present in commercial fuels is scarce [8]. In particular, the adequacy of common sulfur model compounds, such as H_2S, for the simulation of heterocyclic sulfur compounds in commercial low-sulfur fuels is in need of evaluation.

In this work, we consider the suitability of sulfur-containing commercial fuels as primary fuel for solid oxide fuel cell (SOFC) applications and as H_2 source. ZrO_2-supported Rh, Pt, and RhPt catalysts were studied in ATR of simulated and commercial low-sulfur diesel (<10 ppm S). Noble metal catalysts tolerate sulfur better than the conventional Ni-based reforming catalysts [15]. It is also proposed that the catalyst support acts as a sulfur adsorbent when the interaction of the support (i.e. CeO_2) with sulfur is more favorable than reactions between the noble metal and sulfur [15]. ZrO_2, as a bifunctional support, is a promising choice [22,23], because the tolerance to sulfur varies with the acidic properties of the support [16]. For comparative purposes, heterocyclic 4,6-DMDBT and H_2S were used as sulfur model compounds in ATR of simulated fuels (S 10 ppm).

2. Experimental conditions

2.1. Catalyst preparation

Mono- (Rh and Pt) and bimetallic (RhPt) catalysts were prepared by dry impregnation and dry co-impregnation of metal precursors on ZrO_2 support (MEL Chemicals EC0100, 0.25–0.42 mm, calcined at 900 °C for 16 h) to give not more than 0.5 wt% noble metal. The target Rh/Pt molar ratio of the bimetallic catalyst was 2.0 [14]. The catalyst preparation procedure is reported in detail elsewhere [13,14]. After the impregnation and drying, the catalysts were calcined at 900 °C (1 h).

2.2. Catalyst characterization

Characterization of the catalysts has been described previously [14]. The amounts of carbon and sulfur in the catalyst samples were determined with a Leco SC-444, where the carbon and sulfur were burnt from the catalyst sample in O_2 at 1350 °C. The analytical error of the procedure was ±5%.

2.3. Catalyst testing

The activity and stability of the catalysts were studied in autothermal reforming of simulated and commercial hydrocarbon fuels. The reactants consisted of the fuel, water, and air. The simulated fuels, designated as DT and MHT, contained n-dodecane (D, 99+ %, Sigma–Aldrich), methylcyclohexane (M, ≥99.5%, Fluka), n-heptane (H, 99%, Sigma–Aldrich), and toluene (T, ≥99.7% Riedel-de Haën) in molar ratios D/T = 80/20 and M/H/T = 50/30/20, respectively. In addition, H_2S (0.5% in N_2, Aga) or 4,6-DMDBT (97 wt%, Aldrich) was fed to the reactor to give 10 ppm of S in the simulated fuels (DT and MHT). The commercial fuel (low-sulfur

diesel, <10 ppm S) with the aromatic content of 17.4 wt% was provided by Neste Oil Corporation. The density for diesel was measured to be 0.824 g/cm^3.

The amount of catalyst sample tested was 0.2 g. The flow rates of the liquid fuel and water to the reactor were 0.038 and 0.149 g/min, respectively. The total flow rate of the reactants, including O_2, was 300 cm^3/min (NTP) and the flow was diluted with inert gas (Ar or N_2) to give a total flow rate of 900 cm^3/min (NTP) (gas hourly space velocity, GHSV = 3.1×10^5 1/h). The steam to carbon (H_2O/C) and O_2/C molar ratios were 3 and 0.34 mol/mol, respectively. The studied temperature range (400–900 °C) for the ATR system was selected on the basis of thermodynamic equilibrium calculations performed with HSC Chemistry 5.11 [12]. The experimental setup is described in detail elsewhere [14]. After the experiment, the reactor was flushed with Ar or N_2 and cooled down to room temperature.

2.4. Product analysis and calculations

The water and higher hydrocarbons in the product stream were condensed and the dry gas flow (H_2, CO, CO_2, CH_4, and O_2) was analyzed with an extractive gas analyzer (S 710, Sick Maihak Inc.). Dräger ampoules capable of detecting H_2S in amounts from 0.5 to 15 ppm were used to determine the presence of H_2S in the wet and dry flows. In the presence of H_2S, the color of the Dräger-ampoule changes from white to light brown (HgS) due to the following reaction:

$$H_2S + Hg^{2+} = HgS + 2H^+ \tag{6}$$

The element balances were determined from the analyzed product distribution and the measured dry gas flow. The product distribution was calculated with the following equation

$$n_i \, (\%) = \frac{F_i}{\sum_{j=1}^{n} F_j} \times 100 \tag{7}$$

where F_i is the molar flow of the product i. Water was considered as feedstock although water is converted as well as produced in side reactions of ATR.

The conversion of O_2 was calculated from the analyzed feed and product flows (Eq. (8)), and the conversions of simulated and commercial fuels (X_F) and water (X_{H_2O}) were calculated from the amounts of H_2, CO, CO_2, and CH_4 produced and the molar feed flows (Eqs. (9) and (10))

$$X_{O_2} \, (\%) = \frac{F_{O_2,in} - F_{O_2,out}}{F_{O_2,in}} \times 100, \tag{8}$$

$$X_F \, (\%) = \frac{(F_{CO,out} + F_{CO_2,out} + F_{CH_4,out})/x_F}{F_{F,in}} \times 100, \tag{9}$$

$$X_{H_2O} \, (\%) = \frac{(2F_{H_2,out} + 4F_{CH_4,out} - r_F x_F X_F F_{F,in})}{2F_{H_2O,in}} \times 100, \tag{10}$$

where x_F is the average carbon number and r_F the average H/C molar ratio of the fuel (F): $x_{diesel} = 16$ and $r_{diesel} = 1.9$, $x_{DT} = 11$ and $r_{DT} = 2.0$, and $x_{MHT} = 7$ and $r_{MHT} = 1.9$. The accuracy of these calculations was estimated by the error% of the oxygen balance:

$$\text{error}\% = \frac{(2F_{O_2,in} - (F_{CO,out} + 2F_{CO_2,out} + 2F_{O_2,out} + (1 - X_{H_2O})F_{H_2O,in}))}{2F_{O_2,in}}$$
$$\times 100\% \tag{11}$$

In the molar ratio of reforming to oxidation (Ref/Ox; Eq. (12)), which is calculated from the product distribution, the presence of
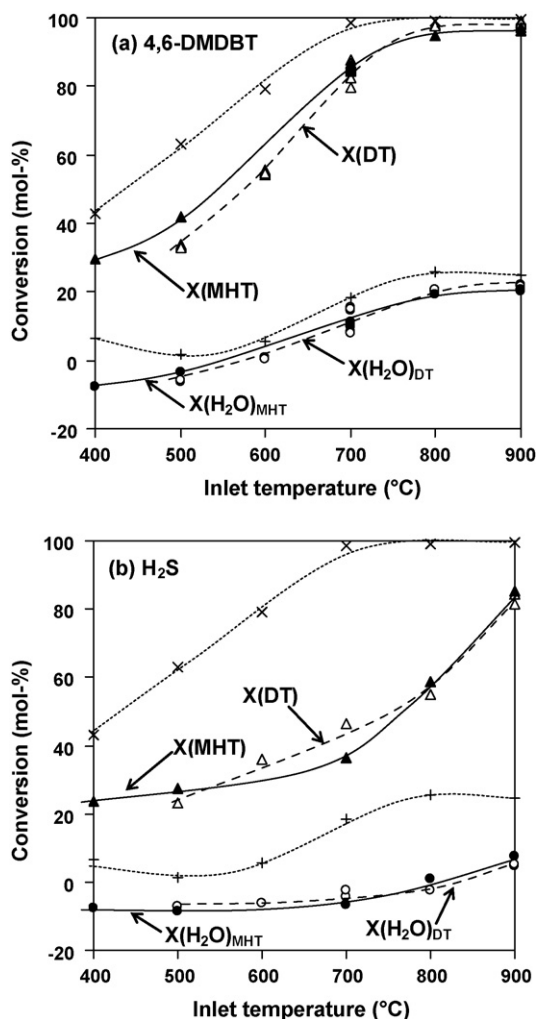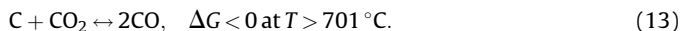
Fig. 2. Effect of 4,6-DMDBT and H_2S on the conversions (X_i) (oxygen (▲), fuel (□), water (○)) and dry product flows (mmol/min) in ATR of simulated (DT) and commercial (diesel) low-sulfur fuel on $RhPt/ZrO_2$ catalyst. Conditions: 700 °C, $H_2O/C = 3$ mol/mol, $O_2/C = 0.34$ mol/mol, S 10 ppm.

low-sulfur diesel. Experiments were performed with the $RhPt/ZrO_2$ catalyst at inlet temperatures of 400–900 °C.

There were only slight differences in conversions between the DT and MHT mixtures studied in ATR in the presence of 4,6-DMDBT (Fig. 1a) and H_2S (Fig. 1b) on the $RhPt/ZrO_2$ catalyst. Thus, the length of the hydrocarbon chain in the fuel or the type of the aliphatic hydrocarbon did not appear to be a critical parameter when studying the reforming of liquid hydrocarbons in the presence of sulfur. In contrast to this, a clear difference was observed between the sulfur compounds (compare Fig. 1a and b).

3.1.1. 4,6-DMDBT

The sulfur-free simulated fuel (DT) corresponded well to the commercial diesel, as can be seen in Fig. 2. The addition of 4,6-DMDBT improved the correspondence, as the conversions and product distribution obtained in ATR of simulated fuels in the presence of 4,6-DMDBT were similar to those of low-sulfur diesel (Fig. 2). The presence of this sulfur compound caused slight deactivation of the bimetallic catalyst with time, since the conversions of DT and water (Fig. 1a) and the amount of hydrogen decreased (Fig. 2) as compared with the sulfur-free conditions where the catalyst was stable [14]. The effect of 4,6-DMDBT on the catalyst performance was not marked, besides H_2S was not detected in the product flow at any time studied (400–900 °C). The error% (Eq. (11)) calculated for experiments performed with 4,6-DMDBT was between −2.5% and +1.6%.

3.1.2. H_2S

The presence of H_2S (S 10 ppm) had a noticeable effect on the performance of the bimetallic catalyst. The conversions of the fuel and water decreased drastically, the fuel conversion being incomplete over the whole temperature range (Fig. 1b). The conversion of O_2 (100%), in contrast, was not affected (Fig. 2). Hence, the presence of H_2S did not hinder the oxidation reactions but only degraded the activity for reforming. Evidently, oxidation reactions were taking place either in the gas phase or on different active sites of the catalyst than SR, whereas the SR reactions can only take place on active sites. It should be added that in our previous studies in sulfur-free conditions, the conversion of O_2 was incomplete on the pure ZrO_2 support, but 100% in the presence of either Rh or Pt [14]. The noble metals must therefore play a critical role in the oxidation reactions, and the oxidation is mainly taking place on the active site.

Fig. 1. ATR conversions (X_i) of simulated fuels (DT (△), MHT (▲)) and water (in ATR of DT (○) and MHT (●)) on $RhPt/ZrO_2$ catalyst in the presence of (a) 4,6-DMDBT and (b) H_2S. Conditions: $H_2O/C = 3$ mol/mol, $O_2/C = 0.34$ mol/mol, S 10 ppm. Conversions of MHT (×) and water (+) obtained in ATR of MHT in sulfur-free conditions are presented for comparative purpose.

the WGS reaction (Eq. (3)) is neglected [13]. The Ref/Ox ratio therefore indicates the real catalyst selectivity for the reforming reactions (SR and POX):

$$\text{Ref/Ox} = \frac{n_{H_2} + n_{CO}}{n_{H_2O} + n_{CO_2}} \tag{12}$$

The CO/CO_2 molar ratio, on the other hand, indicates the importance of the WGS reaction (Eq. (3)) and the Boudouard equilibrium reaction (Eq. (13)):

$$C + CO_2 \leftrightarrow 2CO, \quad \Delta G < 0 \text{ at } T > 701 \text{ °C.} \tag{13}$$

3. Results and discussion

3.1. Evaluation of simulated fuels as models for commercial fuels

ATR of the simulated fuels (DT or MHT) was investigated with H_2S and 4,6-DMDBT as sulfur compounds (S 10 ppm), and the results were compared with those for ATR of the simulated fuels performed in sulfur-free conditions and ATR of the commercial
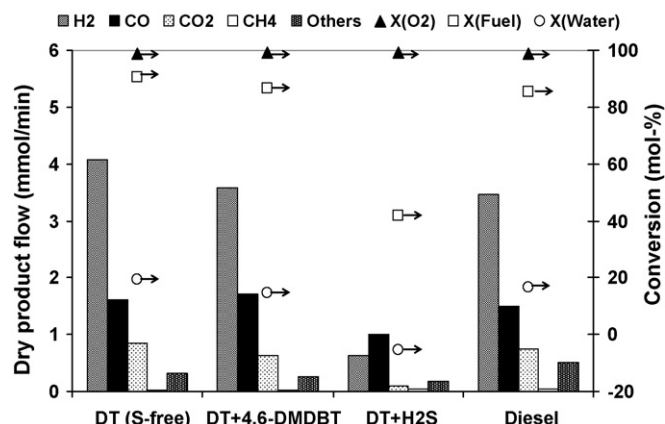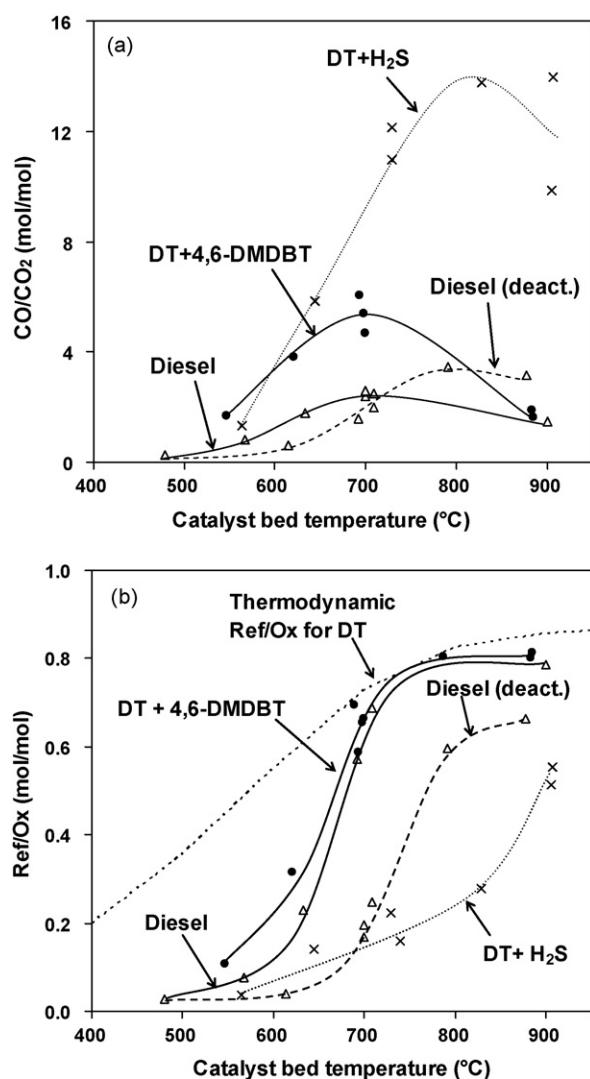
Fig. 3. (a) CO/CO_2 molar ratio and b) Ref/Ox molar ratio ((H_2 + CO)/(H_2O + CO_2)) of the ATR product flows of the commercial diesel ($\triangle$) and simulated (DT) fuels in the presence of 4,6-DMDBT ($\bullet$) and H_2S ($\times$). Conditions: RhPt/ZrO_2, H_2O/C = 3 mol/mol, O_2/C = 0.34 mol/mol, S 10 ppm. For diesel: active catalyst (solid line), deactivated catalyst (dash line).

The conversions of fuel and water in the presence of H_2S were similar to those obtained on the pure support or in thermal cracking reactions performed in sulfur-free conditions without a catalyst [14], that is, mostly H_2 oxidation to H_2O took place resulting in the negative conversion of water. The production of CH_4 increased (Fig. 2) and benzene was detected in the product. Thus, the presence of H_2S also promoted the decomposition of toluene with the cleavage of the methyl group, as favored by the thermodynamics. At temperatures below 700 °C, the reforming activity of the bimetallic RhPt catalyst was almost lost. The catalyst activity improved with temperature (800–900 °C), however, and simultaneously the amount of thermal cracking products decreased (data not reported). Indeed, the same hydrocarbon conversion was obtained at 900 °C in the presence of H_2S as was obtained at 700 °C in sulfur-free conditions or in the presence of the heterocyclic sulfur compound (4,6-DMDBT) (Fig. 1).

To determine whether the influence of H_2S was reversible or irreversible, we turned off the H_2S flow after 6 h on stream. The catalyst activity recovered rapidly. The product distribution and the conversion levels at 700 °C did, however, not reach the values obtained in sulfur-free conditions but corresponded well to those obtained after 6 h on stream in the presence of 4,6-DMDBT. Hence, the deactivation in the presence of H_2S was mainly reversible, but also irreversible deactivation was perceived. The calculated error% (Eq. (11)) for experiments performed with H_2S was between −3.2% and +2.6%.

3.1.3. Product distribution in the presence of sulfur

As can be seen in Fig. 2, the different sulfur compounds had a clear effect not only on the conversions but also on the product distribution. Both H_2S and 4,6-DMDBT decreased the amount of CO_2 produced (Fig. 2), thereby increasing the CO/CO_2 ratio of the product. The effect of H_2S was stronger (Fig. 3a). As depicted in Fig. 3a, in the presence of H_2S the CO/CO_2 ratio also increased dramatically with temperature, having its maximum at 800 °C, whereas with 4,6-DMDBT the ratio had its considerably lower maximum already at 700 °C.

The product distribution and the CO/CO_2 ratio in the product are affected by several equilibrium reactions. To clarify their contribution, we investigated the presence of the WGS (Eq. (3)) and Boudouard (Eq. (13)) reactions. According to thermodynamic calculations, the WGS reaction equilibrium shifts from H_2 + CO_2 to H_2O + CO at temperatures beyond 815 °C, and the Boudouard reaction equilibrium shifts from C + CO_2 to 2CO at temperatures beyond 701 °C. The high CO/CO_2 molar ratio obtained in the presence of H_2S is in agreement with this. In the presence of sulfur, moreover, the CO/CO_2 ratio appeared to increase with time, suggesting a change in the catalyst structure and increased carbon deposition. At temperatures beyond 673 °C, the deposited carbon can also be removed by SR:

$$C + H_2O \leftrightarrow CO + H_2, \quad \Delta G < 0 \text{ at } T > 673\,°C \tag{14}$$
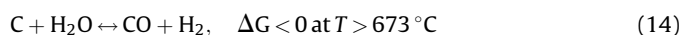
Besides the reforming reactions, H_2 is also produced in side reactions, the WGS reaction (Eq. (3)) being the most important. Indeed, the product distribution suggests that the WGS reaction was present in ATR of both the simulated and commercial fuels. On the RhPt catalyst, moreover, the WGS reaction seems to be stronger in the presence of sulfur than in sulfur-free conditions [13,14]. The amount of H_2 produced does not, therefore, directly reflect the catalyst selectivity for reforming.

The Ref/Ox molar ratio (Eq. (12)) reveals the catalyst selectivity toward reforming reactions (SR and POX) since the effect of the WGS reaction is neglected [13]. Similar values for the Ref/Ox ratio were obtained in ATR of the simulated fuels in sulfur-free conditions and with 4,6-DMDBT and in ATR of low-sulfur diesel. As shown in Fig. 3b, in the presence of heterocyclic sulfur compounds the Ref/Ox ratio predicted by the thermodynamics was reached at 700 °C. The Ref/Ox ratio was noticeably lower when H_2S was used as the sulfur compound; the presence of H_2S degraded both the reforming activity and selectivity, and the oxidation reactions predominated (X_{O_2} = 100%) over the entire temperature range studied. At inlet temperatures below 900 °C, moreover, the catalyst bed temperature was higher than the inlet temperature, indicating an overall exothermic reaction in the presence of H_2S.

Table 1
Conversions and dry product distribution in ATR of low-sulfur diesel (Neste Oil Corp.) on ZrO_2-supported mono- and bimetallic RhPt catalysts after 1 h on stream (700 °C, H_2O/C = 3 mol/mol, O_2/C = 0.34 mol/mol)

	Conversion (mol%)				Product distribution (mol%)			
	Diesel	H_2O	O_2	H_2	CO	CO_2	CH4	Others
Rh	72	8.3	99	46	29	6.9	0.5	17
RhPt	77	19	99	55	26	11	0.5	7.0
Pt	25	−5.8	97	7.7	17	34	2.8	39

3.2. Catalyst activity and stability in ATR of low-sulfur diesel

Rh, Pt, and RhPt catalysts were preliminarily studied to determine the roles of Rh and Pt in the catalyst performance during ATR of low-sulfur diesel. The stability of the RhPt catalyst was then evaluated in ATR of the diesel at inlet temperatures between 400 and 900 °C.

3.2.1. Comparison of Rh, Pt, and RhPt catalysts

Table 1 presents the conversions and dry product distributions obtained on Rh, Pt, and RhPt catalysts at 700 °C. The conversions were highest on the bimetallic catalyst, while the low conversions obtained on Pt, with the formation of thermal cracking products (designated as "others" in Table 1), indicated low reforming activity. The differences between these two catalysts were similar to those described [13,14] for ATR of liquid hydrocarbons in sulfur-free conditions. As expected, on Pt the formation of H_2O in OX was higher than its consumption in SR resulting in negative conversion of H_2O. Thus, the selectivities for reforming products (H_2 and CO) were lower, and the amount of CO_2 was high. The $(H_2 + CO_2)/(H_2O + CO)$ ratio of the product reveals that the catalytic activity for the WGS reaction (Eq. (3)) was highest on the bimetallic RhPt catalyst.

At 700 °C, where the hydrocarbon conversion was incomplete (<80%), deactivation was noticed with time (data not reported). Indeed, activation of all three catalysts was observed in the beginning, but slight deactivation was apparent after just 1 h on stream. The conversion of diesel on the Rh and Pt catalysts deteriorated from 72% and 25% to 55% and 21.5%, respectively. Hence, the deactivation was not as marked for the less active Pt as for the Rh catalyst, although the O_2 conversion decreased from 97% to 89% on Pt and not at all on Rh. Strong sintering occurs on Pt [14], which reduces the concentration of the active $Pt–ZrO_2$ interface [24]. Owing to the high amounts of thermal cracking products (Table 1), carbon deposition may have blocked active sites on the Pt catalyst. The catalyst deactivation also affected the product distribution. On Rh, for instance, the selectivity for H_2 decreased from 50% to 37%, while the selectivity for thermal cracking products increased from 10% to 24% during the 4 h on stream.

On all catalysts, the conversions and product distribution improved with temperature. As shown in Fig. 4, at 900 °C the conversions of diesel and O_2 were almost complete (99–100%) on the RhPt catalyst, and the selectivity for CO_x and the Ref/Ox molar ratio (Eq. (12)) remained constant throughout the experiment (5 h). The product distribution and the conversion of water, on the other hand, changed along the run, as can be seen from the CO/CO_2 and the reverse WGS $((H_2O + CO)/(H_2 + CO_2))$ molar ratios, which increased linearly with time. Since the selectivity for CO_x remained constant, the Boudouard reaction (Eq. (13)) was not causing the shift in the CO/CO_2 ratio. The reverse WGS reaction (Eq. (3)), where the moles of formed CO and consumed CO_2 are equal, must have been taking place instead. Furthermore, the formation of water in the reverse WGS explains the decrease in the water conversion. During the 5 h on stream, the production rates of H_2, CO_2, CO, and H_2O changed with time as follows: −3.2, −2.4, +2.0, and +2.6 mmol/($g_{cat} s^2$), respectively. This change in the catalyst selectivity indicates a change in the catalyst structure or even catalyst deactivation, which in the long-run experiments could affect the catalyst stability. The shift of the WGS reaction toward $CO + H_2O$ with time was also noticed in ATR of the simulated fuels in the presence of sulfur, but not in sulfur-free conditions [14]. We conclude that it was the presence of sulfur in the diesel that
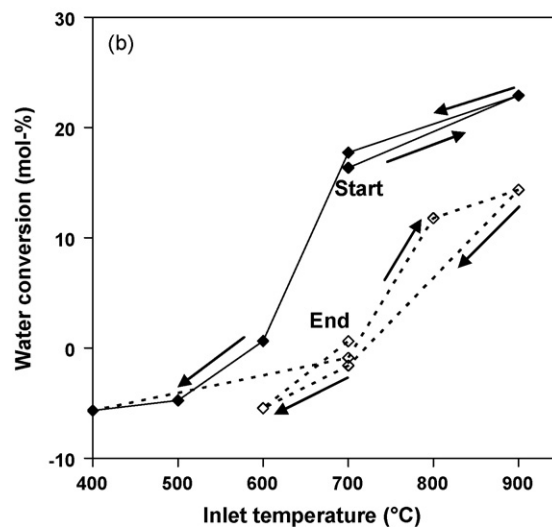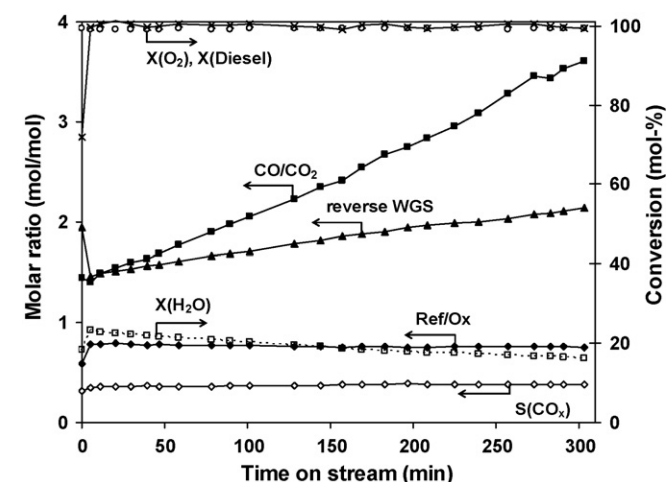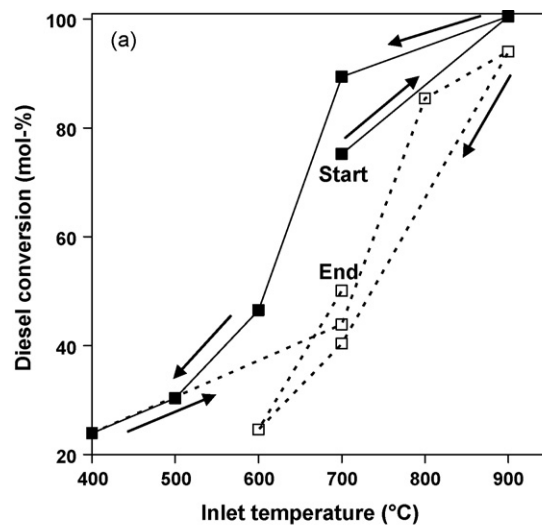

Fig. 4. ATR of low-sulfur diesel on RhPt/ZrO₂ catalyst at 900 °C; conversions (X_i) of diesel (×), water (□), and O_2 (○), and change in the product molar ratios (CO/CO_2 (■), reverse WGS $((H_2O + CO)/(H_2 + CO_2))$ (▲), Ref/Ox $((H_2 + CO)/(H_2O + CO_2))$ (◆), and $S(CO_x)$ (◇)) as a function on time. Conditions: H_2O/C = 3 mol/mol, O_2/C = 0.34 mol/mol.

Fig. 5. Conversion of (a) low-sulfur diesel (■) and (b) water (◆) on RhPt/ZrO₂ catalyst in temperature experiments starting at 700 °C. Conditions: H_2O/C = 3 mol/mol, O_2/C = 0.34 mol/mol. Active catalyst (solid line), deactivated catalyst (dash line).

influenced the catalyst stability. Still, no loss in activity of the bimetallic catalyst was observed at high temperatures (900 °C), where the conversion of the diesel was almost complete (99–100%) (Fig. 4). The high thermal stability of the catalyst was thereby confirmed. In experiments performed with low-sulfur diesel the calculated error% (Eq. (11)) was for all catalysts between −3.8% and +1.3%.

3.2.2. Effect of temperature on catalyst stability

The effect of reaction temperature (400–900 °C) on catalyst activity and stability was studied in ATR of low-sulfur diesel to gain insight into the catalyst deactivation at lower temperatures. This study was performed on Rh and RhPt, the two most active catalysts. The inlet temperature was increased and decreased stepwise between 400 and 900 °C, the initial temperature set point being 700 °C. The two Rh-containing catalysts behaved similarly with temperature. Above 700 °C they were stable, but below 700 °C deactivation occurred. Moreover, the catalyst activity recovered only partly when the temperature was returned to 700 °C, as can be concluded from the conversions of diesel and water presented in Fig. 5 for the RhPt catalyst. Although the conversions and product distribution improved with temperature (900 °C), the initial levels were not recovered. Thus, temperatures above 700 °C are ideal for high reforming activity and selectivity of the Rh-containing catalysts, and irreversible deactivation of the catalyst occurs at lower temperatures.

Catalyst deactivation in the ATR of low-sulfur diesel affected the product distribution and the Ref/Ox ratio (Eq. (12)), but the results obtained on the deactivated RhPt catalyst were better than the corresponding results with the simulated fuels and H_2S (Fig. 3b). Moreover, with the low-sulfur diesel the degraded activity could be partly compensated with rise in temperature.

3.3. H_2S adsorption studies with the RhPt catalyst

In ATR of the simulated fuels (DT and MHT), clear deactivation of the catalyst occurred in the presence of H_2S (Fig. 2). The deactivation was mainly reversible, however, and could be compensated with elevated temperature (Fig. 1b). The effect of temperature on the reversible H_2S adsorption was investigated further. The inlet temperature was increased and decreased stepwise between 500 and 900 °C, the initial temperature set point being 700 °C (Fig. 6). For each temperature, the catalyst bed temperature and the H_2S concentration in the product flow, before (wet) and after (dry) the condenser, were measured (Fig. 6). The inlet temperature was shifted after the conversions and the product distribution stabilized and a steady state was reached.
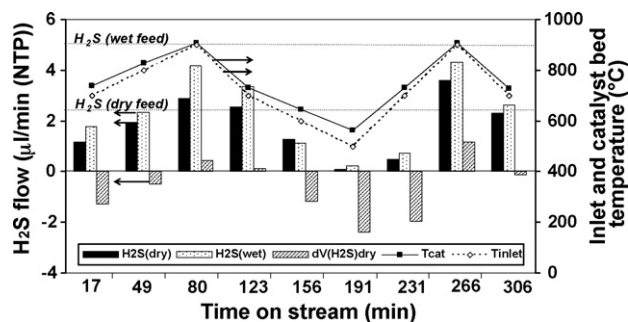
At all temperatures, the amount of H_2S was higher in the wet than in the dry product flow (Fig. 6), revealing that most of the H_2S was caught in the condensed liquid phase. The amount of H_2S in the product changed with the temperature, the accumulation of H_2S being strong at temperatures below 700 °C. When the inlet temperature was increased to 900 °C, the H_2S flow in the dry product was higher than that in the dry feed (2.4 μl/min (NTP)), as can be seen in Fig. 6 (dV represents the difference in the incoming and outgoing H_2S flows). Thus, H_2S was desorbed from the catalyst with elevated temperature, improving the catalyst activity and tolerance against sulfur.

The H_2S adsorption was studied further at 700 °C, where the reactants were fed to the reactor in sequences with and without H_2S, starting with sulfur-free conditions. The sequences were switched after a steady state was reached. When H_2S was added to the feed the conversions of the simulated fuel and water instantly declined (Fig. 7a) and production of the main products decreased (Fig. 7b). The conversions and product distribution subsequently stabilized, and a steady state for the H_2S adsorption was achieved within 10–15 min (Fig. 7a and b). A steady state for the H_2S adsorption was already reached during the first sequence with H_2S. When the H_2S flow was turned off, conversions (Fig. 7a) and the production of H_2, CO, and CO_2 (Fig. 7b) rapidly recovered. The reactivation of the catalyst continued with time; traces of H_2S were detected in the product just 10–20 min after switching off the H_2S flow (Fig. 7a). The initial conversion and product distribution were not regained, however, indicating some irreversible adsorption of the H_2S [20].

Strong catalyst deactivation was caused by reversible sulfur bonding on the RhPt catalyst. However, the catalyst performance
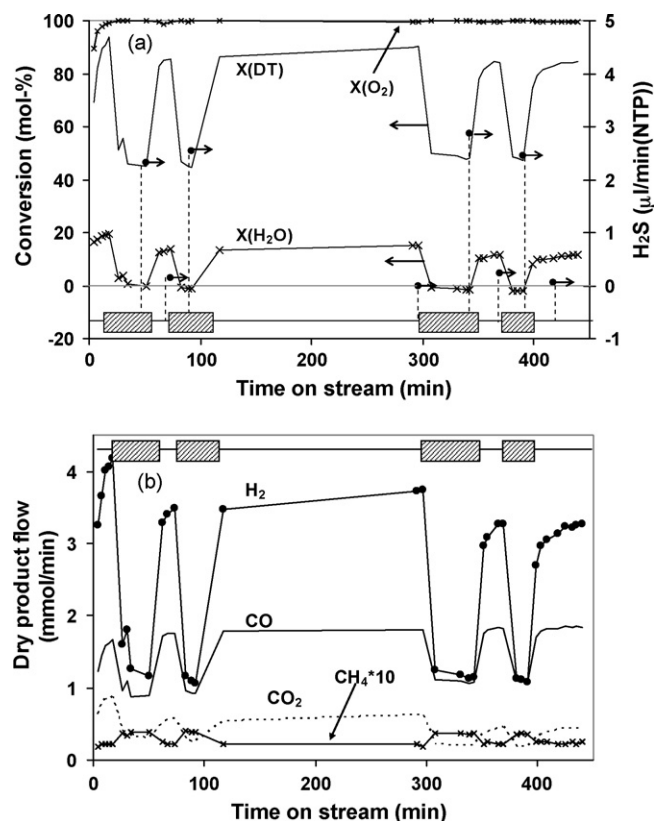

Fig. 7. (a) Conversions (X_i) and (b) dry product flows in ATR of simulated fuel (DT) under the influence of H_2S (S 10 ppm) fed at different times on stream (▨). The measured H_2S flow (μl/min (NTP)) is marked as (●). Conditions: RhPt/ZrO$_2$, 700 °C, H_2O/C = 3 mol/mol, O_2/C = 0.34 mol/mol.

Fig. 6. Inlet temperature (◇), catalyst bed temperature (■), and measured H_2S flow in the dry and wet products of ATR of simulated fuel (DT) on RhPt/ZrO$_2$ catalyst. Conditions: 500–900 °C, H_2O/C = 3 mol/mol, O_2/C = 0.34 mol/mol, S 10 ppm. For the dry flow: $dV(H_2S)_{dry} = V(H_2S)_{out} − V(H_2S)_{in}$ [μl/min (NTP)], $V(H_2S)_{in,dry}$ = 2.4 μl/min (NTP), and $V(H_2S)_{in,wet}$ = 5.0 μl/min (NTP).

Table 2
Sulfur and carbon deposition on the ZrO_2-supported RhPt catalyst tested in ATR of simulated fuel (H_2O/C = 3 mol/mol, O_2/C = 0.34 mol/mol) in the presence of 4,6-DMDBT and H_2S (10 ppm S)

Fuel	Carbon (mg/(gcat h))	Sulfur (mg/(gcat h))	CO/CO$_2$ (average, mol/mol)
MHT	0.95	0.0	2.1
MHT + 4,6-DMDBT	1.2	2.3	2.6
MHT + H$_2$S	0.73	30	3.4

continued stable in the presence of H_2S, as can be seen in Fig. 7, confirming that a steady state prevailed between the sulfur compounds in the gas phase and adsorbed on the catalyst surface. Furthermore, the steady state shifted with temperature.

Reversible adsorption of sulfur species was not observed in the presence of 4,6-DMDBT. Moreover, in ATR performed in the presence of 4,6-DMDBT or with low-sulfur diesel, no H_2S was detected in the wet or dry product flow at any temperature (400–900 °C). This indicates that cracking of the complex heterocyclic compounds (e.g. 4,6-DMDBT) to H_2S and lighter hydrocarbons did not take place, even though this is favored by the thermodynamics [12]. According to thermodynamic calculations, H_2S, S_2O, SO_2, SO_3, and S(s) could form from 4,6-DMDBT in ATR conditions (in the presence of H_2O and O_2), with H_2S the favored product. Unfortunately, neither qualitative nor quantitative studies of such products could be undertaken owing to limitations of the analytical method. Still, we can conclude that since strong catalyst deactivation occurred only when H_2S was added, H_2S must have been the main source of poisoning of the RhPt catalyst, and the catalyst evidently tolerated 4,6-DMDBT or other sulfur compounds formed from 4,6-DMDBT.

3.4. Sulfur and carbon deposition

The sulfur and carbon contents of the three catalysts were determined before and after their use in ATR of the simulated (Table 2) and commercial fuels (Table 3). The amount of sulfur deposited on the RhPt catalyst was low in the presence of heterocyclic sulfur compounds (i.e. 4,6-DMDBT and low-sulfur diesel), and clearly higher in the presence of H_2S (Table 2). Still, just 0.08 wt% of the total sulfur flow (35.7 mgS/(g$_{cat}$ h)) was deposited on the catalyst in the H_2S experiment (5 h), and the sulfur (n_S) to noble metal ($n_{Rh} + n_{Pt}$) molar ratio was only 0.13.

According to visual estimation, the amount of coke deposited on catalyst particles was highest during ATR of low-sulfur diesel, whereas hardly any coke was detected after the experiment with H_2S. This observation was verified by catalyst characterization (see Tables 2 and 3). If we consider the catalyst deactivation and the presence of thermal cracking under the influence of H_2S, the amount of carbon deposited in the H_2S experiment was extraordinarily low. We suggest that the adsorbed sulfur compound, derived from H_2S, either prevented the deposition of carbon by blocking the active sites [2,25] or else promoted certain carbon removal reactions, such as the reverse-Boudouard reaction (Eq. (13)) or SR (Eq. (14)). Indeed, Suzuki et al. [2] showed that
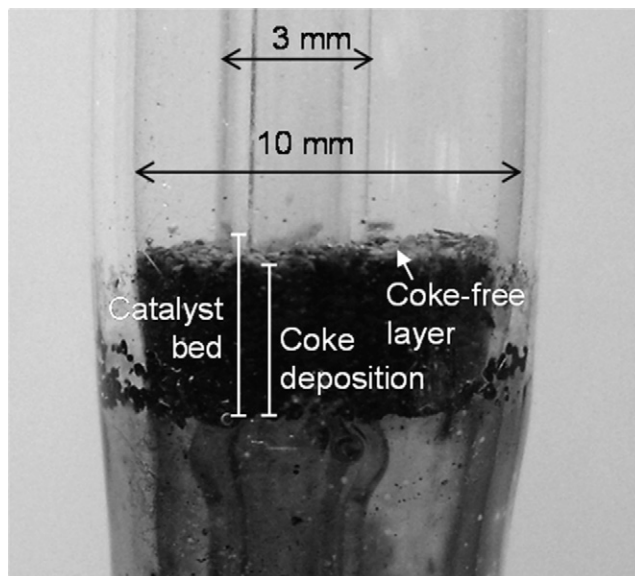

Fig. 8. Photograph of the used RhPt/ZrO_2 catalyst with coke deposition and a coke-free layer. The catalyst was tested in ATR of low-sulfur diesel at 900 °C/5 h. Conditions: H_2O/C = 3 mol/mol, O_2/C = 0.34 mol/mol.

the presence of H_2S prevented CO adsorption on Ru-based catalysts, and similar findings were presented by Strohm et al. [21] for Rh-based catalysts and by Rostrup-Nielsen [25] for Ni-based catalysts. It has also been suggested that the reforming requires a smaller ensemble of active sites than the CO adsorption [21,25,26]. Thus, a certain level of sulfur poisoning minimizes the formation of coke (Boudouard reaction, Eq. (13)) but still allows the steam reforming to proceed [21,25,26]. This would explain the high amount of CO and high CO/CO$_2$ ratio in the product obtained in ATR of the simulated fuels with H_2S (Fig. 3a). Blockage of the active sites would also explain the low conversions and the inhibition of the WGS equilibrium reaction (Eq. (3)).

The large amount of carbon on the RhPt catalyst after ATR of low-sulfur diesel was due to the incomplete conversion of the fuel and to thermal cracking reactions promoting coke formation. The complex nature of commercial fuels, containing polycyclic aromatic hydrocarbons (PAHs), further explains the stronger deactivation of the RhPt catalyst in ATR of low-sulfur diesel than in ATR of simulated fuels in both the presence and absence of sulfur. The average carbon deposition rate increased with temperature from 3.7 mgC/(g$_{cat}$ h) (700 °C) to 4.5 mgC/(g$_{cat}$ h) (900 °C). Two distinct layers were visible in the bimetallic RhPt/ZrO_2 catalyst bed (Fig. 8) after the ATR of low-sulfur diesel at 900 °C (5 h) confirming that coke is partially removed from the catalyst during the ATR. The oxygen seems to assist in the coke removal from the catalyst bed surface especially at high temperatures (900 °C).

Carbon deposition on the three catalysts was visibly different and correlated with the measured amounts of carbon (Table 3). The average carbon deposition on the catalyst bed increased in ATR of low-sulfur diesel in the order Pt > RhPt > Rh, whereas in sulfur-

Table 3
Metal loadings of the ZrO_2-supported mono- and bimetallic RhPt catalysts, and sulfur and carbon deposition after ATR of commercial, low-sulfur diesel (700 °C/5 h, H_2O/C = 3 mol/mol, O_2/C = 0.34 mol/mol)

Catalyst	Rh[a] (wt%)	Pt[a] (wt%)	Carbon (mg/(gcat h))	Sulfur (mg/(gcat h))	CO/CO$_2$ (average, mol/mol)
Rh	0.49	0	2.0	21	4.9
RhPt	0.25	0.22	3.7	5.6	2.2
Pt	0	0.39	4.9	12	0.5

[a] The metal loadings determined by XRF are reported in Kaila et al. [14].

free conditions, the carbon deposition was lowest on the bimetallic catalyst [14]. With low-sulfur diesel, moreover, the amount of carbon was directly proportional to the Pt loading of the catalyst (Table 3), and the CO/CO_2 ratio decreased linearly with increase in the Pt loading.

Comparison of the mono- and bimetallic catalysts showed the amount of deposited sulfur to be clearly highest on the monometallic Rh catalyst and lowest on the bimetallic RhPt catalyst (Table 3). Bitter et al. [24] proposed that the activity of a Pt/ZrO_2 catalyst in CO_2/CH_4 reforming is proportional to the concentration of the Pt–ZrO_2 interface, whereas the activity of a Rh/ZrO_2 catalyst is directly proportional to the availability of Rh sites. For the bimetallic RhPt/ZrO_2 catalyst we earlier found that the metal clusters consist of a Rh_xPt_{1-x} alloy subsurface and an active Rh_2O_3 overlayer [14]. Probably the close interaction between Rh and Pt, similarly to the interaction between Ni and Rh in the steam reforming of jet fuel [21], prevented the binding of the noble metal with the sulfur.

4. Conclusions

H_2-rich fuel gas was successfully produced from low-sulfur diesel (<10 ppm S) on the RhPt/ZrO_2 catalyst. This commercial fuel was simulated with hydrocarbon mixtures (DT and MHT), and the addition of a heterocyclic sulfur compound (4,6-DMDBT, 10 ppm S) improved the similarity. The heterocyclic sulfur compounds present in commercial, low-sulfur diesel (e.g. 4,6-DMDBT) did not significantly affect the activity of the bimetallic catalyst, since the ATR conversions and product distributions were similar to those obtained in sulfur-free conditions. Still, in the presence of sulfur in any form, deactivation of both the mono- and bimetallic catalysts occurred with time.

In ATR of commercial diesel, the carbon deposition increased with the Pt-loading of the catalyst, whereas the sulfur deposition was strongest on the Rh catalyst. Moreover, the carbon deposition decreased in the presence of sulfur, either due to the blockage of active sites, thereby preventing the deposition, or to enhancement of the coke removal reactions. The carbon deposition decreased in the presence of H_2S, even though thermal cracking was present and strong deactivation of the RhPt catalyst was observed.

The catalyst performance was affected drastically by H_2S (10 ppm S). The conversions of simulated fuels and water decreased causing a poor product distribution, while the conversion of oxygen was not affected. After the H_2S flow was switched off, the catalyst activity recovered almost completely owing to the reversibility of the H_2S adsorption. Moreover, H_2S adsorbed strongly on the RhPt catalyst below 700 °C, but desorbed with an increase in temperature. Although the catalyst deactivation in the presence of H_2S (10 ppm S) could be compensated with temperature, complete conversion of the simulated fuel was not achieved at any temperature studied (400–900 °C). Some irreversible deactivation of the Rh-containing catalysts was observed at low temperatures in the ATR of the low-sulfur diesel.

According to these results, ATR of liquid fuels in the presence of sulfur should be performed above 700 °C to avoid RhPt catalyst deactivation. Moreover, owing to the different behavior of sulfur compounds (H_2S and 4,6-DMDBT) and the fact that H_2S is not formed in ATR of low-sulfur diesel nor from 4,6-DMDBT at any temperature, H_2S cannot be considered a suitable model compound for heterocyclic sulfur compounds in commercial, low-sulfur fuels.

Acknowledgment

References

[1] S.K. Bej, S.K. Maity, U.T. Turaga, Energy Fuels 18 (2004) 1227.
[2] T. Suzuki, H.-I. Iwanami, T. Yoshinari, Int. J. Hydrogen Energy 25 (2000) 119.
[3] K. Kirimura, T. Furuya, R. Sato, Y. Ishii, K. Kino, S. Usami, Appl. Environ. Microbiol. 68 (2002) 3867.
[4] X. Rozanska, R. van Santen, F. Hutschka, J. Hafner, J. Catal. 205 (2002) 388.
[5] R.F. Service, Science 305 (2004) 958.
[6] D.L. Trimm, Z.I. Önsan, Catal. Rev.-Sci. Eng. 43 (2001) 31.
[7] L.F. Brown, Int. J. Hydrogen Energy 26 (2001) 381.
[8] D. Shekhawat, T.H. Gardner, D.A. Berry, J.J. Spivey, in: J.J. Spivey, K.M. Dooley (Eds.), Catalysis, vol. 19, Royal Society of Chemistry, London, 2006, pp. 184–253.
[9] R.K. Kaila, A.O.I. Krause, Int. J. Hydrogen Energy 31 (2006) 1934.
[10] P.K. Cheekatamarla, C.M. Finnerty, J. Power Sources 160 (2006) 490.
[11] I. Kang, J. Bae, J. Power Sources 159 (2006) 1283.
[12] A. Roine, HSC Chemistry for Windows 5.11, Outokumpu Research Oy, 2003.
[13] R.K. Kaila, A. Gutierrez, S.T. Korhonen, A.O.I. Krause, Catal. Lett. 115 (2007) 70.
[14] R.K. Kaila, A. Gutierrez, R. Slioor, M. Kemell, M. Leskelä, A.O.I. Krause, Appl. Catal. B (2008), in press.
[15] U. Hennings, R. Reimert, Appl. Catal. B 70 (2007) 498.
[16] H. Yasuda, N. Matsubayashi, T. Sato, Y. Yoshimura, Catal. Lett. 54 (1998) 23.
[17] B.I. Whittington, C.J. Jiang, D.L. Trimm, Catal. Today 26 (1995) 47.
[18] A. Bitsch-Larsen, N.J. Degenstein, L.D. Schmidt, Appl. Catal. B 78 (2008) 364.
[19] A. Qi, S. Wang, C. Ni, D. Wu, Int. J. Hydrogen Energy 32 (2007) 981.
[20] C. Palm, P. Cremer, R. Peters, D. Stolten, J. Power Sources 106 (2002) 231.
[21] J.J. Strohm, J. Zheng, C. Song, J. Catal. 238 (2006) 309.
[22] T. Yamaguchi, Catal. Today 20 (1994) 199.
[23] K. Tanabe, T. Yamaguchi, Catal. Today 20 (1994) 185.
[24] J.H. Bitter, K. Seshan, J.A. Lercher, J. Catal. 176 (1998) 93.
[25] J.R. Rostrup-Nielsen, J. Catal. 85 (1984) 31.
[26] D.L. Trimm, Catal. Today 37 (1997) 233.